Colloid Polym Sci (2007) 285:1407–1410
DOI 10.1007/s00396-007-1718-5

SHORT COMMUNICATION

Preparation of gold colloid using pyrrole-2-carboxylic acid and characterization of its particle growth

PEGylated Gold Colloid as Bionanomaterials

Takeshi Sakura · Yukio Nagasaki

Received: 18 August 2006 / Revised: 10 June 2007 / Accepted: 11 June 2007 / Published online: 26 July 2007
© Springer-Verlag 2007

Abstract Gold colloid was prepared by reduction of tetrachloroaurate using pyrrole-2-carboxylic acid in the presence of α-methoxy-ω-mercaptoethyl-poly(ethylene glycol). The shape and size of the obtained gold colloids were monitored by absorption spectroscopy and transmission electron microscopy during the reduction reaction. In the early stage of the reducing reaction, large fluffy particles with diameters >100 μm were observed. Some of these large particles had rectangular parallelepiped shapes. However, the mean particle size decreased with increasing time. Eventually, these large, non-round-shaped particles disappeared almost completely, and uniform round-shaped particles with a mean diameter of 10.5 nm became dominant.

Keywords Gold nanoparticles · Pyrrole-2-carboxylic acid · α-Methoxy-ω-mercaptoethyl-poly(ethylene glycol) · Particle growth · Bionanosphere

Abbreviations

MeO-PEG-SH	α-methoxy-ω-mercaptoethyl-poly(ethylene glycol)
TEM	transmission electron microscopy
TCA	tetrachloroaurate
PCA	pyrrole-2-carboxylic acid
λ_{max}	plasmon peak wavelength
D_{mean}	mean particle diameter
SD	standard deviation from particle diameter

Introduction

Recently, nanoscale colloidal metal particles have attracted much attention, particularly in the fields of electronics, catalysis, and clinical diagnostics [1–4]. To date, various versatile methods have been reported for gold colloid preparation [5]; most of these methods involve the reduction of tetrachloroauric acid (TCA) using a specific reducing agent, such as citric acid or ascorbic acid. The obtained colloids are stably dispersed in aqueous media by repulsive ionic forces [6–8]. However, for many applications of gold colloids, stabilization by ionic repulsive force is not entirely satisfactory. For example, under the physiological conditions of clinical applications, e.g., immuno-colloidal imaging and diagnostics [9, 10], these gold colloids readily aggregate due to compensation of the electrostatic repulsive force by high ionic strength.

In this report, we describe a method for the preparation of stable gold colloids that have poly(ethylene glycol) (PEG) tethered chains on the surface, which improve both the nonfouling properties and dispersion stability [11, 12]. Using this method, the size distribution of the obtained gold colloid was rather broad as a result of uncontrolled

Electronic supplementary material The online version of this article (doi:10.1007/s00396-007-1718-5) contains supplementary material, which is available to authorized users.

T. Sakura · Y. Nagasaki (✉)
Tsukuba Research Center for Interdisciplinary Materials Science,
University of Tsukuba,
Tennoudai 1-1-1, Tsukuba,
Ibaraki 305-8573, Japan
e-mail: nagasaki@nagalabo.jp

T. Sakura
e-mail: sakura@transparent.co.jp

Present address:
T. Sakura
R&D Division, Transparent Co. Ltd.,
Kashiwanoha 5-4-19,
Kashiwa 277-0882, Japan

reduction mediated by a strong reducing agent, i.e., sodium borohydrate or hydroxylamine. Based on the mild reactivity of pyrrole-2-carboxylic acid (PCA) for the reduction of the aurate cation [13], a monodispersed gold colloid with a PEG tethered chain on the surface was prepared, using PCA as the reducing agent in the presence of mercapto-ended PEG. The formation profile of the gold colloid during the reducing reaction was monitored, and the formation mechanism under these conditions is discussed.

Experimental

Materials

Preparation of gold colloid using PCA in the presence of mercapto-ended PEG

All of the glassware and PTFE-coated magnetic stirring beads were first cleaned with aqua regia, followed by successive rinses with copious quantities of distilled water. An aliquot (9.6 ml) of 50 mM PCA in aqueous solution (99% purity; Aldrich) was added to a 76.8-ml aliquot of 10 mM α-methoxy-ω-mercaptoethyl-poly(ethylene glycol) (MeO-PEG-SH; M_n 5,200, M_w/M_n=1.02; NOF Co. Ltd.). The pH values of these two solutions were adjusted to 10 and 13, respectively, by the addition of NaOH before mixing. To this mixture, 9.6 ml of an aqueous solution of 10 mM TCA (99.95% purity; Wako Pure Chemical Industries) was added with vigorous agitation at room temperature.

Measurements

The UV-vis spectra were monitored using the Shimadzu UV 2400PC. For transmission electron microscopy (TEM), a 6-μl aliquot of the sample solution was pipetted onto carbon-coated, 200-mesh copper grids (Okenshoji), and the surplus solution was removed with filter paper. This procedure was performed in a −80 °C freezer to quench the reduction reaction, and was completed within 30 s. TEM was carried out at 200 kV in the JEOL JEM-2010F apparatus. The particle diameters were determined using the Image Pro Plus software version 5.0 (Media Cybernetics). The diameters of approximately 250 particles were included in the calculations. The zeta potential as a function of time was measured by using ELS 6000 (Photal).

Results and discussion

Selvan and Nogami have reported oxidative polymerization of pyrrole in the presence of TCA [13]. Simultaneously, the TCA, as the initiator, was reduced to form anisotropic gold colloid. Thus, the pyrrole derivatives show a good ability to reduce aurate cations. To prepare a PEGylated gold colloid under mild reduction conditions, we employed PCA as the reducing agent.

Within 1 min of the addition of PCA to the TCA aqueous solution under alkaline conditions in the presence of mercapto-ended PEG, the color of the solution changed from pale yellow to colorless but retained its transparency. The color of the solution gradually changed from gray to purple and, finally, to red. The reduction of TCA by PCA was monitored by UV-vis spectroscopy. Figure 1 shows the time-course of the absorption spectrum of the reaction mixture. The absorption intensity increased along with bathochromic shift as a function of time. At the start of the reaction, plasmon peak wavelength (λ_{max}) was approximately 570 nm, with very low absorption intensity. In the first 40 min of the reaction, λ_{max} based on the surface plasmon peak shifted from 570 to 526 nm along with an increase in the peak intensity. The color of the solution at 40 min was pale gray–purple. After 40 min, the absorption increased significantly, while λ_{max} was shifted slightly from 526 to 521 nm. This downward shift of λ_{max} indicates that the ratio of larger particles to smaller particles decreased, in accordance with Kreibig's theory [14].

It is well known that the λ_{max} of the plasmon peak of gold colloid correlates with its size, i.e., a longer wavelength denotes a larger particle size in this region. The observed blue shift as a function of the reaction time indicates that the mean size of most of the obtained gold nanoparticles decreased as a function of time.

To obtain information on particle size, direct observation was carried out with TEM. Figure 2 shows the TEM images of the obtained gold colloids at the different reaction times. Most of the obtained colloids were fluffy in shape and ca.

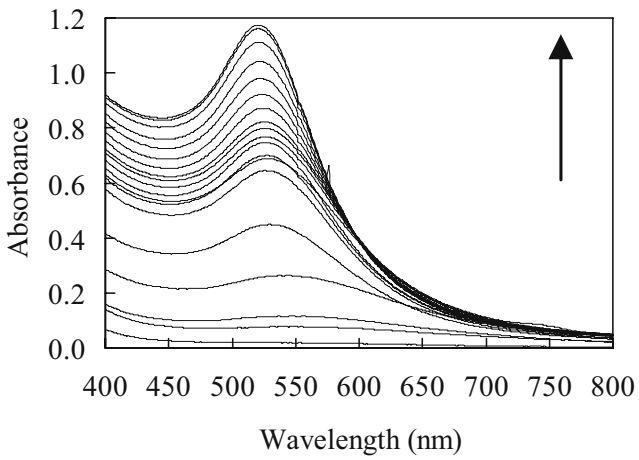

Fig. 1 UV-vis spectra as a function of reaction time recorded at 2, 5, 10, 20, 30, 40, 45, 50, 60, 80, 100, 120, 180, 300, 540, 1,320, 2,940, 4,320, and 5,820 min from the bottom to the top, respectively

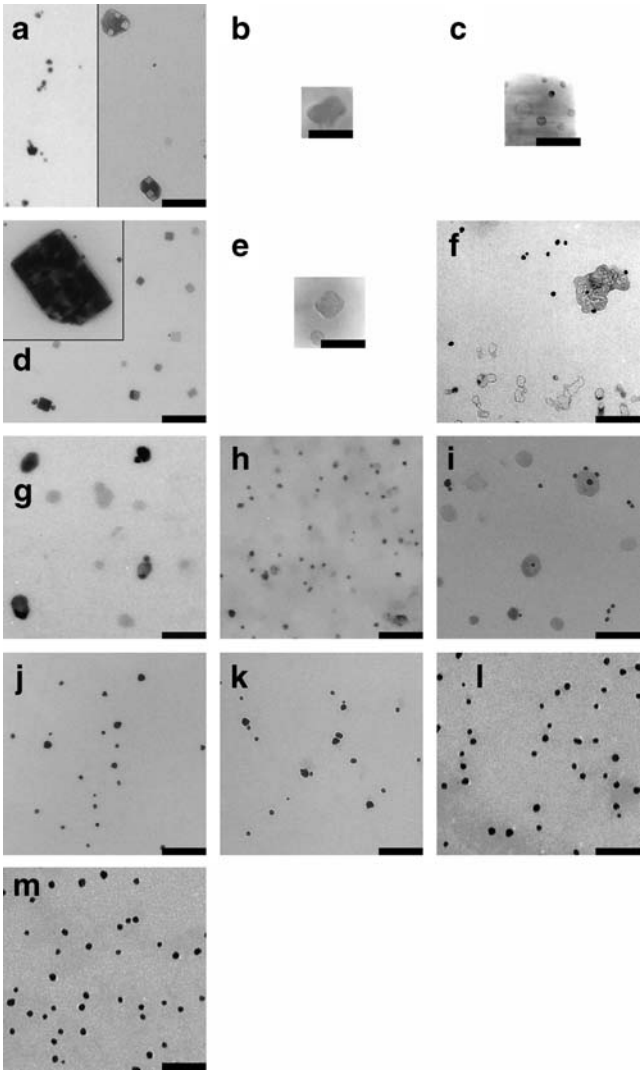

Fig. 2 TEM images of the particles in a reaction quenched samples at **a** 20 min, **b** 20 min, **c** 20 min, **d** 40 min, **e** 40 min, **f** 120 min, **i** 540 min, **j** 1,320 min, **k** 2,940 min, and **m** 5,820 min, respectively. The *black scale bar* corresponds to 100 nm

100 nm in diameter at the 20-min time point (Fig. 2a–c). The colloids obtained after 40 min had the same shape but were smaller in size compared to those obtained after 20 min (Fig. 2d–e). After 40 min, spherical colloids of almost identical diameter (10–30 nm) were observed (Fig. 2f–m).

We also investigated the crystal structures of the large fluffy particles shown in Fig. 2b and e, which appeared to have low electron density. The electron diffraction spectroscopy image (Fig. 3) clearly indicates that these particles have {1, 0, 0} face. Thus, these particles have crystal structures.

The kinetics of the changes in mean particle diameter (D_{mean}) and standard deviation (SD) thereof calculated from the TEM images are shown in Fig. 4 (the details of the size frequency changes as a function of time are given in the

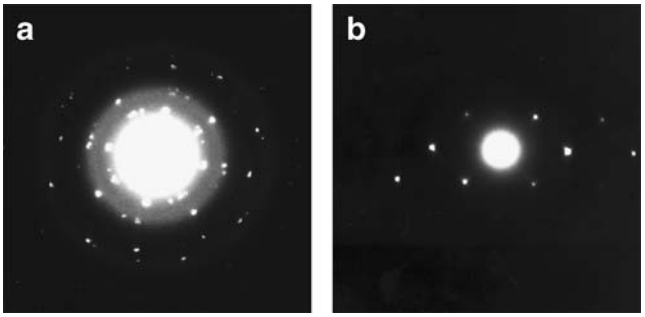

Fig. 3 Electron diffraction of **a** the large fluffy particle in Fig. 2b and **b** rectangular parallelepiped and cubic particles in Fig. 2e, respectively. The above electron diffraction indicates that both of these particles have {1,0,0} face. Thus, the particles have crystal structures

supporting information). These data demonstrate that D_{mean} decreased with increasing time and eventually became uniform at 10.5±2.6 nm (D_{mean} ± SD). These D_{mean} changes are in good agreement with the results of the time-course changes in the spectrum values.

For the preparation of gold colloid via the reduction of TCA, the following three main mechanisms have been proposed: (1) La Mer has proposed the burst nucleation model [6, 15, 16], in which homogeneous nucleation occurs until the nucleus attains a critical size. In this type of solution, the colloid precursor is consumed rapidly during burst nucleation, and the concentration of aurate ions falls below the supersaturation level. The nuclei then grow at the same speed, with the limitation of diffusion, and eventually become uniform particles. (2) An agglomeration mechanism has been proposed by Uyeda et al. [17], who observed

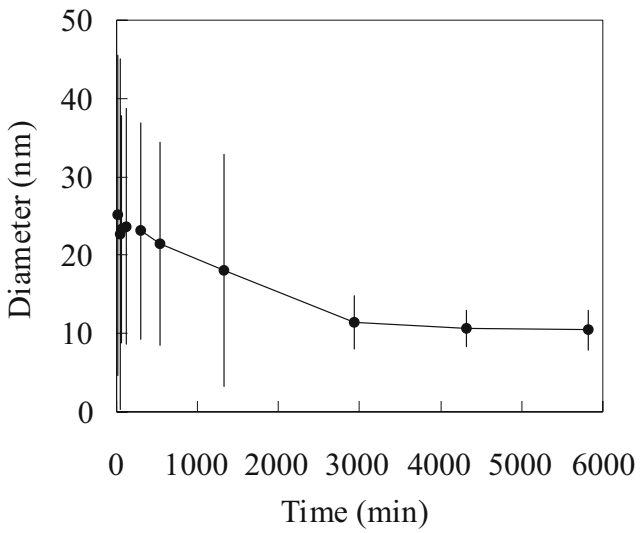

Fig. 4 Mean particles diameters (D_{mean}, *dots*) and the particles size SDs (which are expressed by *vertical bars*) plotted as a function of time. Relatively large particles are formed in the initial stage of the particles generation and small particles become dominant during the course of time

smaller elementary crystallites for most of the gold nanoparticles, which are commonly referred to as Faraday, Weimarn, and sodium citrate sols. They also found that particles were formed by parallel or radial twins with definite mutual orientations, which they attributed to a nuclear interaction at the early stage of the reduction reaction. They assumed that metastable nuclei with the icosahedral configuration grow into multiple twins and eventually transit to natural cube-octahedral nuclei, which grow into parallel twins due to mutual interactions. (3) Chow and Zukoski have described the formation of large fluffy particles [18], which form at an early stage of the reaction and subsequently fell apart due to increased surface potential, thereby producing the uniform gold particles. The newly produced small particles are stabilized by repulsive electrostatic forces.

Based on the data obtained from the TEM images (Fig. 2), it appears that reactions governed by two different growing mechanisms take place. In the first mechanism, large fluffy particles (Fig. 2a, b) are produced at the early stage of the reaction, while at the end of the reduction reaction, small round-shaped particles of diameter 10.5 nm predominate. These large fluffy particles appear to be less electron dense than the small particles. In addition, they contain some quadrilateral structures, which appear to be precursors for the subsequent rectangular parallelepiped or cubic particles. Most of the particles observed at 40 min of the reaction were rectangular parallelepiped or cubic in shape (Fig. 2d, e), and these square particles were almost completely absent in the sample taken at 60 min. In the second mechanism, the continuous production of nuclei and their growth during the reaction are evidenced by the increase in Abs_{525}. The theoretical mechanisms underlying the particle growth seen in our experiments are currently under investigation and will be published elsewhere.

Interestingly, D_{mean} decreased with increasing time, while the surface potential was almost neutral and constant (between −3.6 and +3.4 mV) during the reaction period (Fig. 4). The latter phenomenon, a relatively small change in surface potential, was not observed in the experiment conducted by Chow and Zukoski, who concluded that the large fluffy particles seen at the early stage of the reaction consisted of agglomerates of the very small particles, which subsequently fell apart as a result of the increase in surface charge related to adsorption of the citrate ion [18]. In general, four strategies are used to stabilize particles: the use of an organic ligand, electrical repulsion, steric repulsion, and amphipathic molecules [19]. In the present study, the gold nanoparticles were stabilized by adsorbing MeO-PEG-SH to the surface.

Conclusions

Our study shows the coexistence of two mechanisms for the formation of particles. The first mechanism is the classical burst-nucleation model and the second mechanism is similar to the model proposed by Chow. The production of large fluffy particles with diameters >100 nm was observed in the early stage of the reduction reaction. At the end of the reduction reaction, small uniform particles 10.5 nm in diameter became dominant. The driving force for the fragmentation of these large particles in Chow's experiment was the increase in surface potential. In our experiment, large fluffy particles were also observed. However, the driving force behind the changes in the mean size of the particles observed in our experiments is presumed not to be electric repulsion based on the measurements of particle surface potential. We believe that MeO-PEG-SH is adsorbed onto the surface of the particles at the early stage of the reduction reaction, and that this tethered PEG diminishes the changes in surface potential.

Acknowledgements The authors thank Mr. Ichihara (University of Tokyo) for helpful discussions and assistance with this research.

References

1. Musick MD, Keating DC, Keefe MH, Natan MJ (1997) Chem Mater 9:1499
2. Toshima N, Wang Y (1994) Adv Mater 6:245
3. Abraham GE, Himmel PB (1997) J Nutr Environ Med 7:295
4. Huang MF, Kuo YC, Huang CC, Chang HT (2004) Anal Chem 76:192
5. Hayat MA (1989) (ed) Colloidal gold, principles, mwthods and applications. Academic, San Diego
6. Turkevich J, Stevenson PC, Hiller J (1951) Discuss Faraday Soc 11:55
7. Stathis EC, Fabrikanos A (1958) Chem Ind 27:860
8. Frens G (1973) Nat Phys Sci 241:20
9. Sokolov K, Follen M, Aaron J, Pavlova I, Malpica A, Lotan R, Richards-Kortum R (2003) Cancer Res 63:1999
10. Paciotti G, Myer L, Weinreich D, Goia D, Pavel N, McLaughlin R, Tamarkin L (2004) Drug Deliv 11:169
11. Otsuka H, Akiyama Y, Nagasaki Y, Kataoka K (2001) J Am Chem Soc 123:8226
12. Sakura T, Takahashi T, Kataoka K, Nagasaki Y (2005) Colloid Polym Sci 284:97
13. Selvan ST, Nogami M (1998) J Mater Sci Lett 17:1385
14. Kreibig U, Fragstein V (1996) C Z Phys 224:307
15. LaMer VK, Dinger RH (1950) J Am Chem Soc 72:4847
16. Takiyama K (1958) Bull Chem Soc Jpn 31:944
17. Uyeda N, Nishino M, Suito E (1973) J Colloid Interface Sci 43:264
18. Chow MK, Zukoski CF (1994) J Colloid Interface Sci 165:97
19. Yonezawa T, Toshima N (1996) Surface 34:426